Detection of adulteration of alcoholic beverages using near infrared hyper spectral imaging

By

Achiraya Tantinantrakun
Department of Food Science, Faculty of Food-Industry, King Mongkut's Institute of Technology Ladkrabang, Chalongkrung Road, Ladkrabang, Bangkok 10520, Thailand
Email: 63608025@kmitl.ac.th

Kittithanon Suwapanichkittikorn
Department of Food Science, Faculty of Food-Industry, King Mongkut's Institute of Technology Ladkrabang, Chalongkrung Road, Ladkrabang, Bangkok 10520, Thailand

Keivalin Jindaruang
Department of Food Process Engineering, Faculty of Food-Industry,King Mongkut's Institute of Technology Ladkrabang, Chalongkrung Road, Ladkrabang, Bangkok 10520, Thailand

Chantharalak roekkathok
Department of Food Process Engineering, Faculty of Food-Industry,King Mongkut's Institute of Technology Ladkrabang, Chalongkrung Road, Ladkrabang, Bangkok 10520, Thailand

Pradit Kiawphan
Department of Food Process Engineering, Faculty of Food-Industry,King Mongkut's Institute of Technology Ladkrabang, Chalongkrung Road, Ladkrabang, Bangkok 10520, Thailand

Rachit Suwapanich
Department of Food Science, Faculty of Food-Industry, King Mongkut's Institute of Technology Ladkrabang, Chalongkrung Road, Ladkrabang, Bangkok 10520, Thailand

Anthony Keith Thompson
Cranfield University, College Road, Cranfield, Bedford, MK43 0AL, United Kingdom
Email: keiththompson28@yahoo.com

Sontisuk Teerachaichayut
Department of Food Process Engineering, Faculty of Food-Industry,King Mongkut's Institute of Technology Ladkrabang, Chalongkrung Road, Ladkrabang, Bangkok 10520, Thailand
Email: sontisuk.te@kmitl.ac.th

Abstract

Adulteration of alcoholic beverages creates problems to both commerce and consumers. A rapid, accurate and reliable technique for detecting the adulterated of alcoholic beverages would be highly beneficial. Near infrared hyperspectral imaging (NIR-HSI) in the wavelength range of 935-1720 nm was tested in order to predict the adulteration in alcoholic beverages by quantitative and qualitative analysis. Denaturalization of an alcoholic beverage, using a blend of ethanol with isopropyl alcohol (EI), was tested as an adulterant in this study. It was added into an alcoholic beverage at various percentages. For quantitative analysis, partial least squares regression (PLSR) was used to develop the calibration model for predicting the percentage EI in the adulterated beverages. Smoothing spectral pretreatments were tested for establishing the calibration model. Accuracy for EI prediction gave a correlation coefficient

(Rp) of 0.852 and root mean square error of calibration (RMSEP) of 18.25%. For qualitative analysis, partial least squares-discriminant analysis (PLS-DA) was used to develop the classification model for discriminating the pure alcoholic beverages from the adulterated alcoholic beverages. The smoothing and standard normal variate transformation (SNV) spectral pretreatment was used for establishing the classification calibration model. Accuracy of classification using leave-one- out cross-validation (LOOCV) was 90.71%. Therefore, it was concluded that NIR-HSI has potential to be used for both the prediction of EI in adulterated alcoholic beverages as well as the level of contamination.

Index Terms— calibration, prediction, model, quantitative, qualitative, isopropyl alcohol

Introduction

Many types of alcohol have been used by mankind from time immemorial for medical, industrial and leisure purposes. All alcohols are toxic to some degree, depending on the type and amount consumed, also tolerance to toxicity varies between people. Ethanol is the alcohol used in drinks, which is produced from fermentation of sugars, followed by distillation for spirits. Other alcohols are used for other purposes, for example isopropanol and methanol are applied externally to people to control ailments and ethylene glycol is used in cars as an antifreeze. Adulteration of alcoholic beverages is a centuries old problem [1], [2]. [3] reported that in Mexico authorities were searching for the source of adulterated alcohol that had recently killed 46 people, who had bought and drunk the spirit to celebrate Mother's Day and to attend a funeral. [4] reported that spirits, which had been adulterated with methanol, resulted in the deaths of many people in India, China and Malaysia. In 1985, several Austrian companies illegally adulterated their wines with diethylene glycol to make them appear sweeter and more full-bodied. In Thailand alcoholic beverages have been contaminated with isopropyl alcohol, which is commonly used, often combined with ethanol, as an anti-bacterial agent for sterilization surfaces such as instruments, tools and human [5]. Mass spectrometry was reported to be a method of detecting congeners in whiskey, but its use is destructive, expensive and time consuming [6]. Therefore, a non-destructive fast accurate and reliable technique for detecting the adulteration in alcoholic beverages would be a great asset to the industry as well as ensuring safety for the consumer.

There are research reports that studied non-destructive techniques to detect the adulteration in liquid foods, such as olive oil by using mid-infrared, UV–visible and fluorescence spectroscopy [7], sesame oil by using fluorescence spectroscopy [8], flaxseed oil by using near-infrared spectroscopy [9], mustard oil by using Fourier transform infrared spectroscopy [10], coconut oil by using Fourier transform infrared spectroscopy [11], [12] honey by using nuclear magnetic resonance [13] and grape syrup by using dielectric spectroscopy [14].

NIR-HSI, a non-destructive technique combines spectral spectroscopy and image processing. NIR-HSI has been successfully used for detecting the quality of various foods non-destructively including: hens' eggs [15], cakes [16], limes [17], kiwifruit [18], [19], tomatoes [20], mulberry [21], grapes [22], loquat fruit [23], strawberries [24], oranges [25], peanuts [26], wheat kernels [27], maize [28], okra [29] and cheese [30]. NIR-HSI can also be used to analyze the distribution of chemical within samples and was used for detecting the adulteration in tapioca starch [31]. Therefore NIR-HSI was tested for use in detecting adulteration in alcoholic beverages in this study.

Materials and Methods

Samples preparation

A good brand name vodka (containing 40% ethanol) were purchased from a reliable liquor stores that were used as the alcoholic beverages in this study. The contaminant, ethanol with isopropyl alcohol (EI) was prepared by mixing 99.9% ethyl alcohol and 99.9% isopropyl alcohol in the ratio of 99 to 1 (v/v). For quantitative analysis, EI was adjusted to the same concentration as the vodka and the EI was added to the vodka in different concentrations from 0 to 100% (v/v). 120 samples were used for quantitative analysis. Samples of vodka (n=20) were prepared from different bottles, giving the total number of samples of 140 for qualitative analysis. Each sample was placed in a glass bottle, which was closed with a cap and rubber seal and stored in an air-conditioned room at 25°C about 24 hours, then 3 mL of each sample was poured into a transflectance cup for measurement.

Spectral Data Acquisition

Each sample was scanned using a push-broom-laboratory-based sisu CHEMA system with a hyperspectral camera (Specim Fx17, Spectral Imaging Ltd, Oulu, Finland) in the wavelength range of 935–1720 nm at the scanning speed of 15 mm/s. A dark reference was measured while the shutter was closed and the black lid was covered on the camera. A white reference was measured before every scanning using a Spectralon bar.

Data analysis

For quantitative analysis, the total number of samples (n=120) were divided into 2 sets: a calibration set (n=80) and a prediction set (n=40). The calibration set was used for establishing the calibration model using partial least squares regression (PLSR). The dependent variables were the percentage of EI that was added to the vodka and the independent variables were the spectra of the samples. Spectral pretreatment methods (smoothing, 1st derivative, 2nd derivative, standard normal variate (SNV), multiplicative scatter correction (MSC) and combined methods) were used in order to obtain the optimal conditions, by testing the correlation coefficient of cross validation (R_{cv}), the root mean square error of cross validation (RMSECV) and latent variables (LV). The performance of the calibration model was determined from the correlation coefficient of calibration (R_c), the root mean square error of calibration (RMSEC) and the LV. The accuracy of the calibration model was determined from the correlation coefficient of prediction (R_p), the root mean square error of prediction (RMSEP) and the LV.

For qualitative analysis, the total number of samples (n=140) were divided into 2 groups. The first group was the pure samples (n=20), which were assigned as ''pure'' with the number of 0. The second group was the adulterated samples (n=120) were assigned as "adulterated" with the number of 1. The dependent variable was then either 0 or 1 (''pure'' or "adulterated") while independent variables were the spectra of each sample The spectral pretreatment methods (smoothing, 1st derivative, 2nd derivative, SNV, MSC and combined methods) were determined in order to obtain the best classification model.

Partial least squares discriminant analysis (PLS-DA) was carried out in order to establish a classification model. The cut off value was 0.5. The samples that had the predicted value of less than 0.5 were classified as ''pure'' and the samples that had a predicted value of 0.5 or more were classified as "adulterated". The accuracy of the classification model was determined by the percentage of correct predictions in both groups using LOOCV. Data were analyzed using the Unscrambler X Version 10.5.1 (CAMO, Osla, Norway).

Result and Discussion

Spectra of samples

Spectra of the sample images acquired in the area of 100 x 100 pixels was allocated as the region of interest (ROI), which were selected for each sample. The ROI were then averaged and used as a representative of each sample. The acquired absorbance spectrum of each sample from ROI was ploted (Fig. 1) and its average absorbance spectrum in the wavelength range between 935-1720 nm was used as the independent variable of each sample for analysis.

The absorbance spectra of EI samples, adulterated vodka and pure vodka were averaged and the spectral feature of the average absorbance spectra of three groups was compared (Fig. 2). The average absorbance spectra of three groups showed similar peaks but their absorbance at around 1690 nm were different. Normally, the original absorbance spectra contained spectra of components would overlap, but there were clear peaks of the original spectra clearly showing the peaks of the main components of the samples. The main peak of the original spectra showed in the range of 1460-1600 nm, which had previously been shown to be associated with the hydrogen bands of alcohols (Workman, & Weyer, 2012). The peak at around 1454 nm has also previously been shown to be associated with the first overtones of O-H stretching of water and ethanol [32] with a peak at around 1685 nm indicating the second overtones of C-H stretching and was shown to be associated with aromatic groups [33].
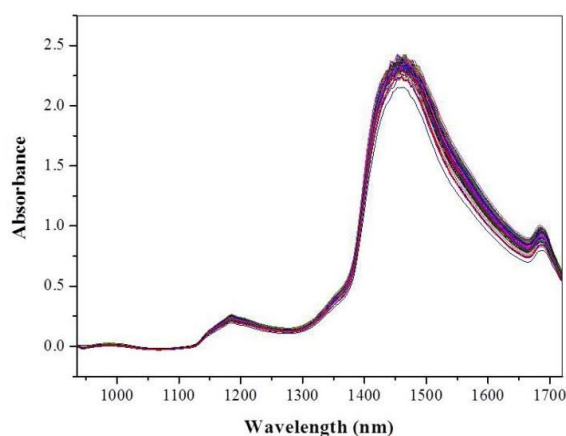

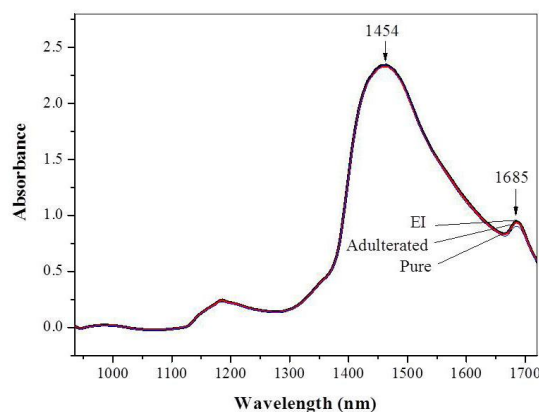**Fig.1.** *The average absorbance spectra of samples*

Fig.2. *The average absorbance spectra of groups: EI samples, adulterated vodka and pure vodka*

Quantitative analysis

For quantitative analysis, the samples were separated into the calibration and the prediction sets. The details of samples in each set, added to various ratio of EI are shown in Table 1. The values of the dependent variable (percentage of EI of samples) in the prediction set were in the range of the calibration set and the standard deviation of EI percentage of samples in the calibration set and the prediction set was similar.

Table 1 *Details of added- EI samples in the calibration set and prediction set*

Item	Calibration	Prediction
Number of samples	80	40
Range (%)	100-0	100-0
Mean (%)	42.53	42.2
Standard deviation (%)	34.45	34.77

Table 2 *PLSR models using various spectral pretreatment methods for predicting percentage of EI in the wavelength range of 935-1720 nm.*

No.	Spectral pretreatments	LV	R	RMSECV (%)
1	original	11	0.792	21.82
2	smoothing	9	0.848	18.17
3	1st Derivative	2	0.420	31.36
4	2nd Derivative	3	0.518	29.93
5	MSC	9	0.631	29.14
6	SNV	11	0.671	27.60
7	smoothing + SNV	7	0.791	21.02

LV = latent variables, Smoothing =Savitzky-Golay smoothing, 1st derivative = Savitzky-Golay first derivative differentiation, 2nd derivative = Savitzky-Golay second derivative differentiation, MSC = multiplicative scatter correction, SNV = standard normal variate transformation, R = correlation coefficient, RMSECV = root mean square error of cross validation.

The smoothing pretreatment method gave the best results for establishing the calibration model for predicting EI percentage in the region of 935-1720 nm (R_{cv}= 0.848, RMSECV= 18.17%) (Table 2). Therefore, the spectral pretreatment using smoothing was used to establish the calibration model for predicting EI percentage in this study.

Table 3 *PLSR model for predicting the percentage of EI in the calibration set and the prediction set by spectra in the region of 935-1720 nm.*

Pre treatment	LV	Calibration			Prediction		
		n	R_c	RMSEC (%)	n	R_p	RMSEP (%)
Smoothing	9	80	0.921	13.31	40	0.852	18.25

n = the number of samples, LV = latent variables, R_c =the correlation coefficient of calibration, R_p =the correlation coefficient of prediction RMSEC represent root mean square error of calibration, RMSEP represent root mean square error of prediction.

The calibration model for predicting EI percentage gave good correlation (Table 3) with the PLSR model in the calibration set having R_c= 0.924 and RMSEC= 13.31% and in the prediction set having R_p= 0.852 and RMSEP= 18.25%.
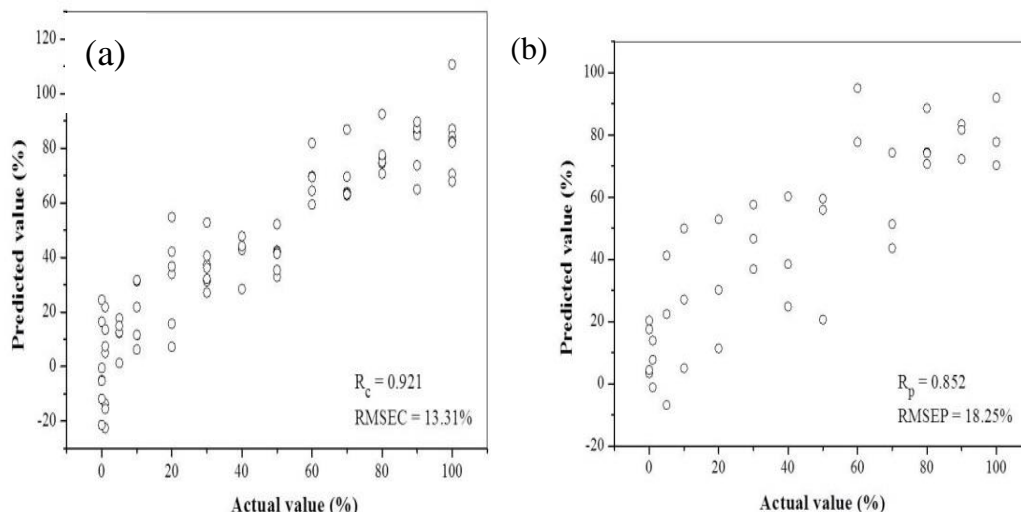
Fig. 3. *The scatter plot of actual and predicted values of EI percentage using the PLSR model.*

The predicted values of percentage of EI from the PLSR model by spectra in the region of 935–1720 nm were compared with the actual values of the percentage of EI in the calibration set (Fig. 3a) and in the prediction set (Fig. 3b). The results showed that the PLSR model had good performance and accuracy for predicting percentage of EI. Therefore. It was clear that using NIR-HSI showed a potential for use in detecting percentage of EI that had been added to vodka.

Qualitative analysis

Absorbance spectra of samples of both adulterated and non-adulterated vodka were used for qualitative analysis. The scores for the plots of the PC1 and PC2 using spectral information of adulterated and non-adulterated vodka showed that the two clusters were completely separated, with the variation for PC1 and PC2 at 96% and 4%, respectively (Fig. 4).
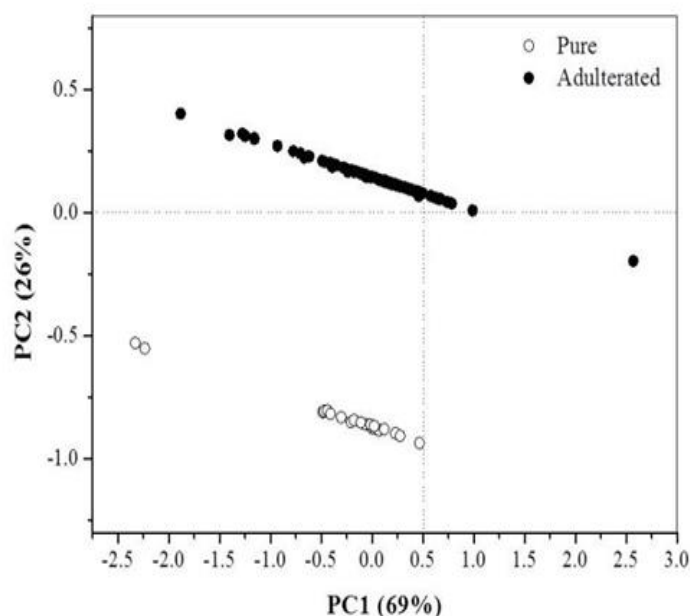

Fig. 4. *Principle component analysis of adulterated vodka and non-adulterated vodka*

Table 4 *Leave-one-out cross-validation of classification models by various spectral pretreatment methods in the wavelength range of 935-1720 nm.*

Spectral pretreatments	n	LV	Pure correct	Pure Incorrect	Adulterated correct	Adulterated Incorrect	Overall Accuracy (%)
Original	140	3	8/20	12/20	115/120	5/120	87.86
Smoothing	140	11	10/20	10/20	114/120	6/120	88.57
1st Derivative	140	3	9/20	11/20	116/120	4/120	89.29
2nd Derivative	140	3	8/20	12/20	115/120	5/120	87.86
MSC	140	3	8/20	12/20	117/120	3/120	89.29
SNV	140	3	8/20	12/20	117/120	3/120	89.29
Smoothing + 1st Derivative	140	3	9/20	11/20	117/120	3/120	90.0
Smoothing + MSC	140	8	10/20	10/20	116/120	4/120	90.0
Smoothing + SNV	140	7	10/20	10/20	117/120	3/120	90.71

n = the number of samples, LV = latent variables, Smoothing =Savitzky-Golay smoothing, 1st derivative = Savitzky-Golay first derivative differentiation, 2nd derivative = Savitzky-Golay second derivative differentiation, MSC = multiplicative scatter correction, SNV = standard normal variate transformation.

The combined methods of spectral pretreatment including smoothing and SNV gave the best results (90.71%) (Table 4). The results of PLS-DA using the classification model had an accuracy of 93.57% by calibration and 90.71% by LOOCV (Table 5).

Table 5 *Classification model by PLS-DA in the calibration set and the prediction set*

Item		The calibration set	LOOCV
N		140	140
Wavelength (nm)		935-1720	935-1720
Spectral pretreatment		Smoothing + SNV	Smoothing + SNV
LV		7	7
Pure group	Correct	12/20	10/20
	Incorrect	8/20	10/20
Adulterated group	Correct	119/120	117/120
	Incorrect	1/120	3/120
% Overall accuracy		93.57	90.71

n = the number of samples, LV = latent variables, LOOCV= Leave-one-out cross-validation, Smoothing =Savitzky-Golay smoothing, SNV = standard normal variate transformation.
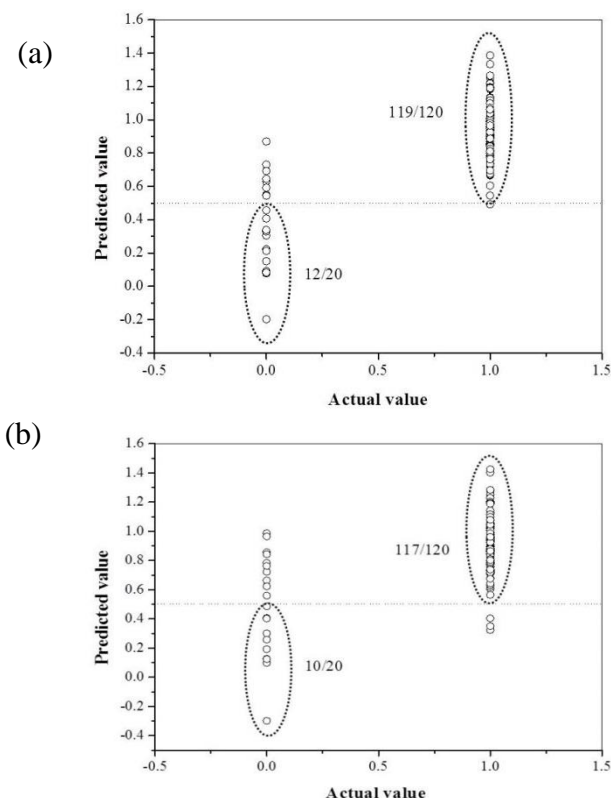
Fig. 5. *The scatter plot of actual and predicted values for classification of pure vodka (0) and adulterated vodka (1): (a) calibration and (b) LOOCV*

The predicted and actual values for classification of non-adulterated vodka (0) and adulterated vodka (1) from the classification model, using PLS-DA by spectra in the region of 935-1720 nm were compared with the cut off value of 0.5, which showed that the classification model had good accuracy for classification (Fig. 5). The performance classification model by calibration was 93.57% (Fig. 5a) and the accuracy of prediction was 90.71% (Fig. 5b) by testing with the model using LOOCV. This showed that NIR-HSI had potential for use in the identification of adulteration in vodka.

Conclusion

It is concluded that near infrared hyperspectral imaging could be successfully used to quantitatively predict the percentage of EI in adulterated vodka. The method used was to establish the calibration model using partial least squares regression. Smoothing spectral pretreatment gave the best results for establishing the calibration model (with transformation spectral pretreatment being the optimum) for establishing the classification model with accuracy of 90.71%. Using partial least squares-discriminant analysis, gave an accuracy (R_p=0.852 and RMSEP =18.25%). Therefore, it is concluded that near infrared hyperspectral imaging could be used for detecting ethyl alcohol with isopropyl alcohol in adulterated vodka.

Acknowledgment

References

Kruse, J.A.. "Methanol and ethylene glycol intoxication. Critical Care Clinics''. 28 (4): 661–711, 2012.

Hess, R, Bartels, M.J., & Pottenger, L.H. Ethylene glycol: "an estimate of tolerable levels of exposure based on a review of animal and human data". Archives of Toxicology. 78 (12): 671–80, 2004.

BBC News. 2020. https://www.bbc.com/news/world-latin-america-52648026 , 22 Nov 2021.

Everstine K. 2020. Fraud in Alcoholic Beverages. https://foodsafetytech.com/column/fraud-in-alcoholic-beverages/ , 22 Nov 2021.

Thairath News. 2014. https://www.thairath.co.th/content/441447 (in Thai), 22 Nov 2021.

Aylott, R. I. & MacKenzie, W. M. "Analytical Strategies to Confirm the Generic Authenticity of Scotch Whisky" J. Inst. Brew. 116, 215–229, 2010.

Uncu, O., & Ozen, B. "A comparative study of mid-infrared, UV–visible and fluorescence spectroscopy in combination with chemometrics for the detection of adulteration of fresh olive oils with old olive oils". Food control, 105, 209–218, 2019.

Yuan, Y. Y., Wang, S. T., Wang, J. Z., Cheng, Q., Wu, X. J., & Kong, D. M. "Rapid detection of the authenticity and adulteration of sesame oil using excitation-emission matrix fluorescence and chemometric methods". Food control, 112, 107145, 2020a.

Yuan, Z., Zhang, L., Wang, D., Jiang, J., Harrington, P. de B., Mao, J., Zhang, Q., & Zhang, Z. "Detection of flaxseed oil multiple adulteration by near-infrared spectroscopy and nonlinear one class partial least squares discriminant analysis". LWT - Food science and technology, 125, 109247, 2020b.

Jamwal, R., Amit, Kumari, S., Balan, B., Dhaulaniya, A. S., Kelly, S., Cannavan, A., & Singh, D. K. "Attenuated total reflectance–fourier transform infrared (ATR–FTIR) spectroscopy coupled with chemometrics for rapid detection of argemone oil adulteration in mustard oil". LWT - Food science and technology, 120, 108945, 2020.

Amit, Jamwal, R., Kumari, S., Dhaulaniy, A. S., Balan, B., & Singh, D. K. "Application of ATR-FTIR spectroscopy along with regression modelling for the detection of adulteration of virgin coconut oil with paraffin oil". LWT - Food Science and Technology, 118, 108754, 2020a.

Amit, Jamwal, R., Kumari, S., Kelly, S., Cannavan, A., & Singh, D. K. "Rapid detection of pure coconut oil adulteration with fried coconut oil using atr-ftir spectroscopy coupled with multivariate regression modelling". LWT - Food Science and Technology, 125, 109250, 2020b.

Song, X., She, S., Xin, M., Chen, L., Li, Y., Heyden, Y. V., Rogers, K. M., & Chen L. "Detection of adulteration in chinese monofloral honey using 1H nuclear magnetic resonance and chemometrics". Journal of food composition and analysis, 86, 103390, 2020.

Naderi-Boldaji, M., Mishra, P., Ahmadpour-Samani, M., Ghasemi-Varnamkhasti, M., Ghanbarian, D., & Zahra, I. "Potential of two dielectric spectroscopy techniques and chemometric analyses for detection of adulteration in grape syrup". Measurement, 127, 518–524, 2018.

Suktanarak, S., & Teerachaichayut, S. "Non-destructive quality assessment of hens' eggs using hyperspectral images". Journal of Food Engineering, 215(1), 97-103, 2017.

Sricharoonratana, M., Thompson, A. K., & Teerachaichayut, S. "Use of near infrared hyperspectral imaging as a non-destructive method of determining and classifying shelf life of cakes". LWT, 136(1), 110369, 2021.

Teerachaichayut, S., & Ho, H. T. (2017). Non-destructive prediction of total soluble solids, titratable acidity and maturity index of limes by near infrared hyperspectral imaging.

Postharvest Biology and Technology, 133, 20-25. doi:https://doi.org/10.1016/j.postharvbio.2017.07.005

Ma, T., Xia, Y., Inagaki, T., & Tsuchikawa, S. "Non-destructive and fast method of mapping the distribution of the soluble solids content and pH in kiwifruit using object rotation near-infrared hyperspectral imaging approach". Postharvest Biology and Technology, 174, 111440, 2021.

Benelli, A., Cevoli, C., Fabbri, A., & Ragni, L. "Ripeness evaluation of kiwifruit by hyperspectral imaging". Biosystems Engineering. doi:https://doi.org/10.1016/j.biosystemseng.2021.08.009, 2021.

Sun, Y., Pessane, I., Pan, L., & Wang, X. "Hyperspectral characteristics of bruised tomatoes as affected by drop height and fruit size". LWT, 141, 110863. doi:https://doi.org/10.1016/j.lwt.2021.110863, 2021.

Yang, L., Gao, H., Meng, L., Fu, X., Du, X., Wu, D., & Huang, L. "Nondestructive measurement of pectin polysaccharides using hyperspectral imaging in mulberry fruit". Food Chemistry, 334, 127614, 2021.

Benelli, A., Cevoli, C., Ragni, L., & Fabbri, A. "In-field and non-destructive monitoring of grapes maturity by hyperspectral imaging". Biosystems Engineering, 207, 59-67, 2021.

Munera, S., Gómez-Sanchís, J., Aleixos, N., Vila-Francés, J., Colelli, G., Cubero, S., Blasco, J. "Discrimination of common defects in loquat fruit cv. 'Algerie' using hyperspectral imaging and machine learning techniques". Postharvest Biology and Technology, 171, 111356, 2021.

Cho, J.-S., Lim, J. H., Park, K. J., Choi, J. H., & Ok, G. S. "Prediction of pelargonidin-3-glucoside in strawberries according to the postharvest distribution period of two ripening stages using VIS-NIR and SWIR hyperspectral imaging technology". LWT - Food Science and Technology, 141, 110875. 2021.

[Riccioli, C., Pérez-Marín, D., & Garrido-Varo, A. "Optimizing spatial data reduction in hyperspectral imaging for the prediction of quality parameters in intact oranges". Postharvest Biology and Technology, 176, 111504, 2021. doi:https://doi.org/10.1016/j.postharvbio.2021.111504

Yuan, D., Jiang, J., Qiao, X., Qi, X., & Wang, W.

"An application to analyzing and correcting for the effects of irregular topographies on NIR hyperspectral images to improve identification of moldy peanuts". Journal of Food Engineering, 280, 109915, 2020.

Zhang, L., Sun, H., Li, H., Rao, Z., & Ji, H. "Identification of rice-weevil (Sitophilus oryzae L.) damaged wheat kernels using multi-angle NIR hyperspectral data". Journal of Cereal Science, 101, 103313, 2021.

da Conceição, R. R. P., Simeone, M. L. F., Queiroz, V. A. V., de Medeiros, E. P., de Araújo, J. B., Coutinho, W. M., . . . de Resende Stoianoff, M. "A. Application of near-infrared hyperspectral (NIR) images combined with multivariate image analysis in the differentiation of two mycotoxicogenic Fusarium species associated with maize". Food Chemistry, 344, 128615, 2021.

Xuan, G., Gao, C., Shao, Y., Wang, X., Wang, Y., & Wang, K. "Maturity determination at harvest and spatial assessment of moisture content in okra using Vis-NIR hyperspectral imaging". Postharvest Biology and Technology, 180, 111597, 2021. doi:https://doi.org/10.1016/j.postharvbio.2021.111597

Calvini, R., Michelini, S., Pizzamiglio, V., Foca, G., & Ulrici, A. "Evaluation of the effect of factors related to preparation and composition of grated Parmigiano Reggiano cheese using NIR hyperspectral imaging". Food Control, 131, 108412, 2022.

Khamsopha, D., Woranitta, S., & Teerachaichayut, S. "Utilizing near infrared hyperspectral imaging for quantitatively predicting adulteration in tapioca starch". Food Control, 123(1), 107781, 2021.

Osborne, B. G., Fearn, T., & Hindle, P. H. "Practical NIR spectroscopy with applications in food and beverage analysis" (2nd ed., p.227). Harlow, Essex, UK: Longman Scientific and Technical, 1993.

Workman, J. and L. Weyer, "Practical Guide and Spectral Atlas for Interpretive Near-Infrared". CRC, 2012.